

# Ultrafast Excited-State Dynamics of Tricarbocyanine Dyes Probed by Two-Dimensional Electronic Spectroscopy: Polar Solvation vs Photoisomerization

Yogita Silori<sup>1</sup>, Pankaj Seliya<sup>1,2</sup> and Arijit K. De<sup>1\*</sup>

<sup>1</sup>Department of Chemical Sciences, Indian Institute of Science Education and Research (IISER) Mohali, Knowledge City, Sector 81, SAS Nagar, Punjab 140 306, India.

<sup>2</sup>Present address: Department of Molecular Spectroscopy, Max Planck Institute for Polymer Research, Ackermannweg 10, D-55128, Mainz, Germany.

\*Email: [akde@iisermohali.ac.in](mailto:akde@iisermohali.ac.in)

## [SI-I]: 2DES setup:

The details of the setup are provided in manuscript (experimental section 2.2.2) and the schematic can be seen in [figure S1](#).

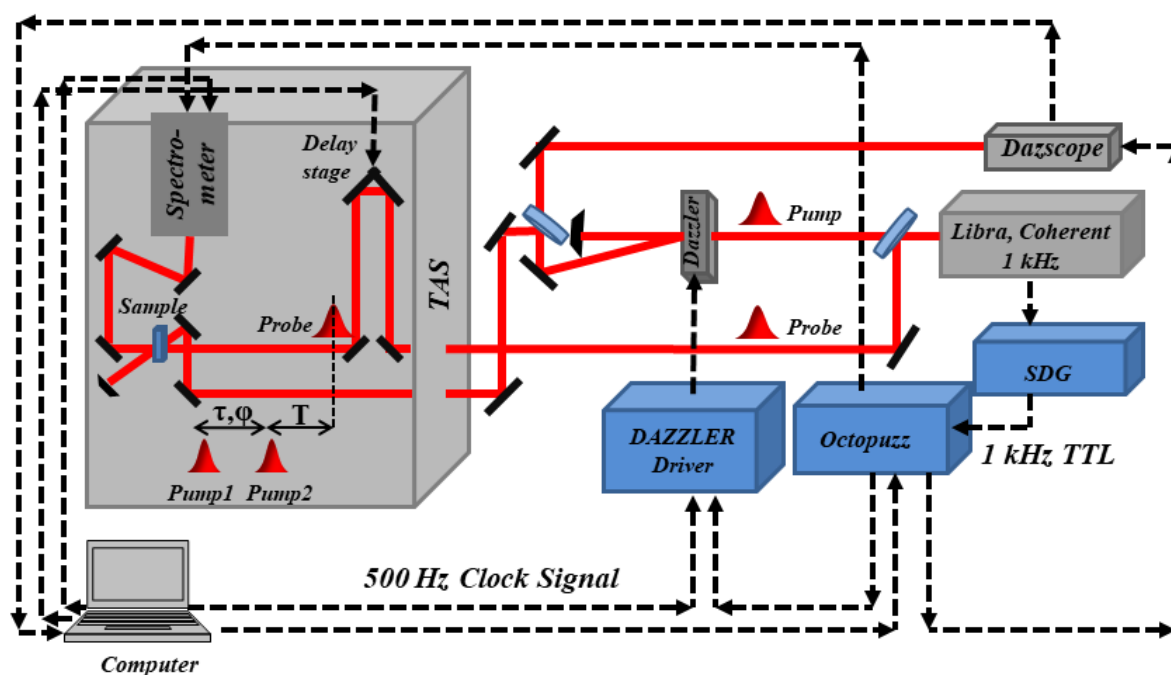


**Figure S1.** Schematic diagram for the 2DES setup, where the pulse shaper integrated in a customized transient absorption spectrometer.

## Supplementary Information

### [SI-II]: Pulse width measurement using FROG analysis:

The intensity autocorrelation data is used to extract phase and amplitude of the pulses using frequency resolved optical gating (FROG) algorithm [1, 2] in order to calibrate the pulse shaper. The free-space pulsewidth (FWHM) is  $\sim 54$  fs as shown in figure S2 (a-c). A cross-correlation between the diffracted pump (by Dazzler, with  $\sim 35$ -40% efficiency) and the probe ( $\sim 54$  fs FWHM) yield a pulsewidth  $\sim 86$  fs for diffracted pump as shown in figure S2 (d-f). A cross-correlation between this pulse-pair and the probe ( $\sim 54$  fs FWHM) yield a pulsewidth  $\sim 99$  fs for each pulse of the pulse-pair as shown in figure S2 (g-i) (note a slight difference in intensities). This clearly indicates that after applying phase/amplitude mask to generate phase-locked pulses, the pulse width increases quite significantly. The algorithm reveals the presence of small cubic phases in all the possible pulses as shown in figure S2.

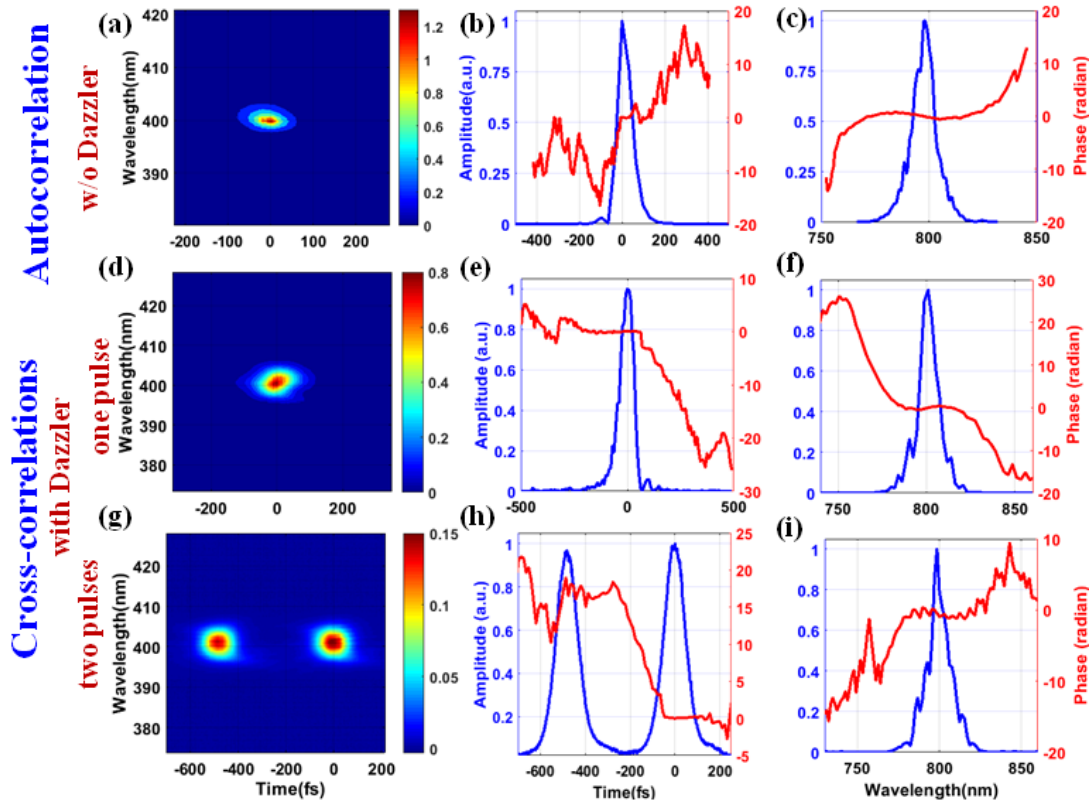


**Figure S2.** Plots for spectrally resolved pulse width profiles with corresponding amplitude and phases of pulses in time and frequency domain using FROG retrieval analysis for the autocorrelation of 800 nm without pulse shaper (a, b, c), with pulse shaper, cross correlation of 800 nm with pulse shaper (g, h, i) and for two pump pulses (j, k, l) in intensity autocorrelation method. Color: blue represents amplitude and red represents phase of the pulse.

## Supplementary Information

### [SI-III]: Signal processing scheme:

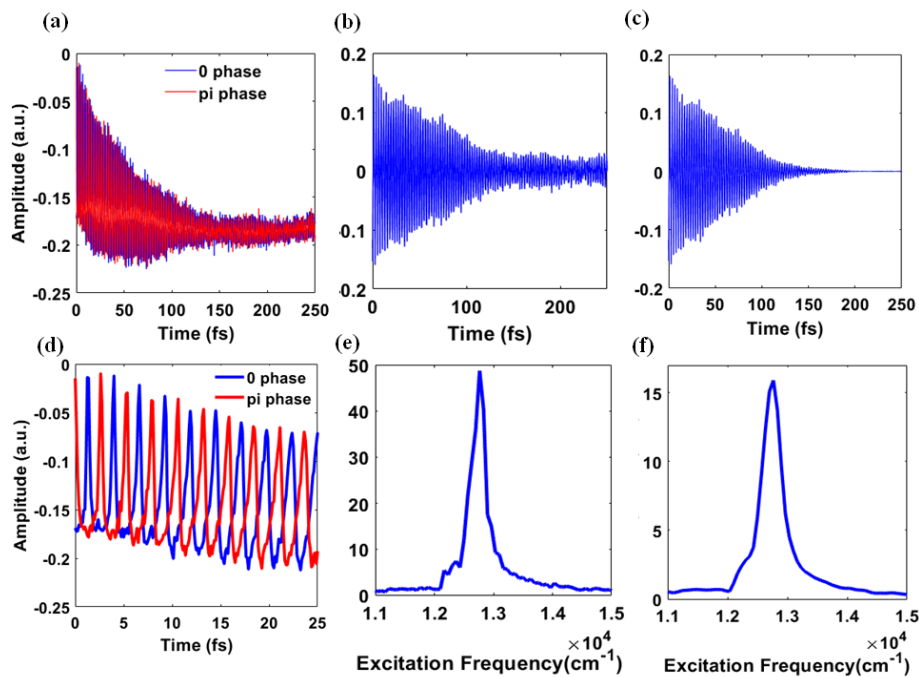


**Figure S3.** Plots of oscillations of signal (a) without phase cycling, (b) with 2-step phase cycling, and (c) after imposing Hanning window function, respectively (top panel). In the bottom panel, (d) shows zoomed in data for 0 and  $\pi$  phases. Plots (e) & (f) show the FFT signal of (b) and (c), respectively.

## Supplementary Information

### [SI-IV]: Spectral evolution of DNTTCI at arbitrary probe delays (T):

The spectral evolution at arbitrary probe delay (T) can be seen in [figure S4](#) of DNTTCI in ethanol and ethylene glycol.

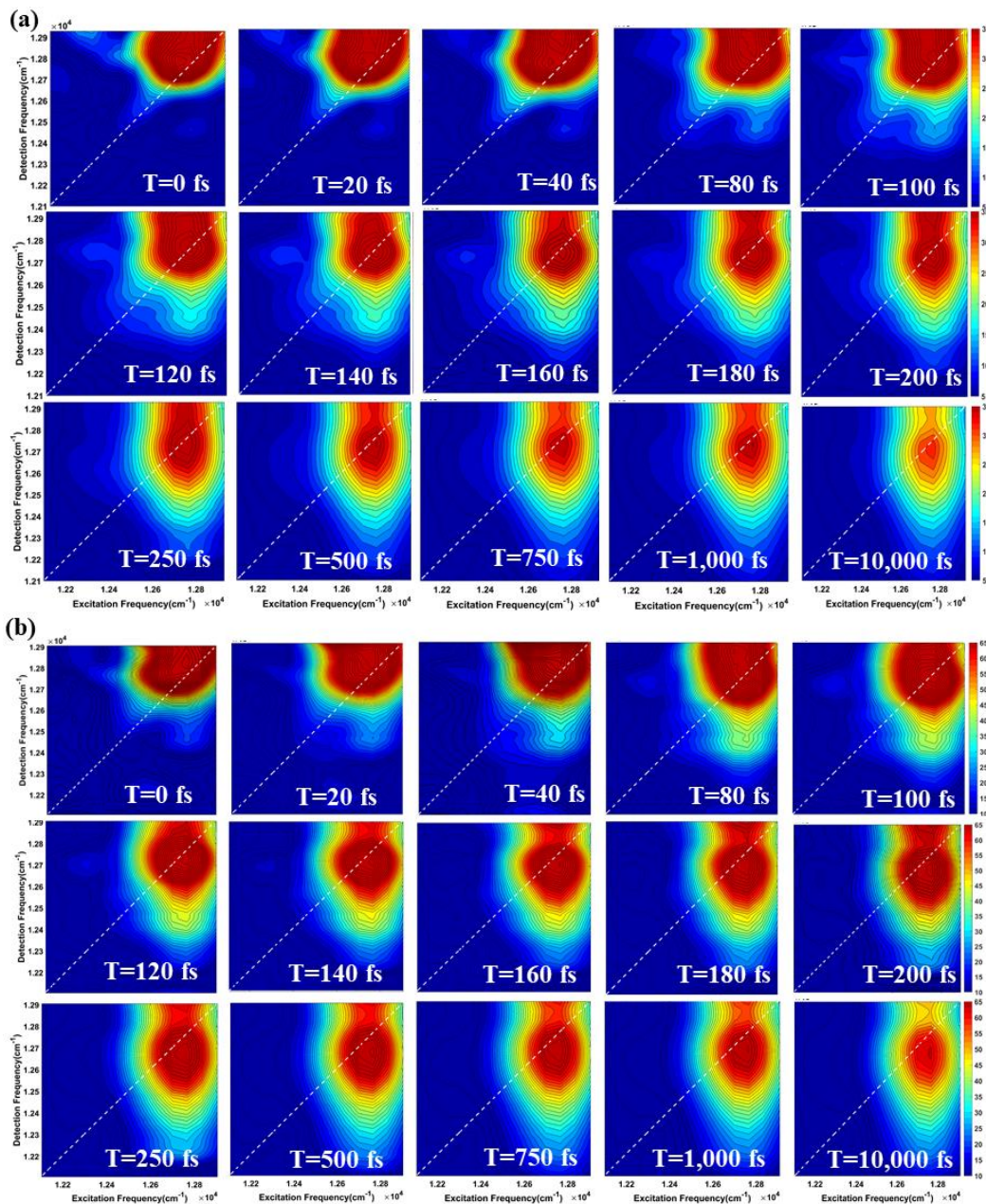


**Figure S4.** Contour plots of 2DES of DNTTCI at various probe delays (T) using 2-step phase cycling scheme in ethanol (top panel (a)) and ethylene glycol (bottom panel (b)).

## Supplementary Information

### [SI-V]: Lognormal fit:

The spectral traces of DNTTCI at various probe delays in both the solvents (ethanol & ethylene glycol) are fitted in lognormal fit (equation 1) as shown in [figure S5](#).

$$y = y_0 + \frac{A}{\text{sqrt}(2*\pi)*w*x*\exp\left(\frac{\left(\ln\left(\frac{x}{x_c}\right)\right)^2}{2*w^2}\right)} \quad (1)$$

where,  $x_c$  denote the central frequency and  $w$  the full width at half maximum of the spectra.

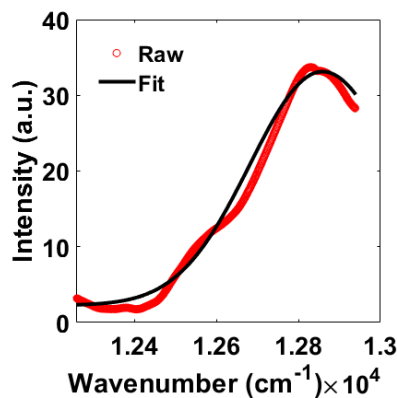


**Figure S5.** Plots of the raw data with corresponding lognormal fit of DNTTCI in ethanol at 0 fs probe delay. Color: blue corresponds to raw data and red lognormal fit.

## Supplementary Information

### **[SI-VI]: Spectral evolution of IR-140 at arbitrary probe delays (T) at different excitation frequencies:**

As discussed in the manuscript ([section 4.2.2](#)), the species A and C show absorption at the same frequency ( $\sim 12,700\text{ cm}^{-1}$ ) while they emit at different spectral regions ( $\sim 12,670\text{ cm}^{-1}$  and  $\sim 12,350\text{ cm}^{-1}$ ). At early time (up to  $\sim 50\text{ fs}$ ) isomer A shows higher emission intensity and above this time scale the intensity decreases significantly whereas the intensity of species B (excited at  $\sim 12,420\text{ cm}^{-1}$ ) increases. At longer probe delay ( $>100\text{ fs}$ ), the intensities of both the species (A & B) decrease and species C increases. Therefore, due to excitation of these species at different frequencies, three slices are taken at different frequency regions along excitation axis ( $12,700\text{ cm}^{-1}$ ,  $12,400\text{ cm}^{-1}$  and  $12,200\text{ cm}^{-1}$ ) to see the stimulated emission dynamics. Excitation at  $12,700\text{ cm}^{-1}$ , shows an isoemissive point in the time resolved emission spectra (TRES) between species A and B at  $\sim 12,440\text{ cm}^{-1}$  ( $T \leq 100\text{ fs}$ ) and then between B and C at  $\sim 12,370\text{ cm}^{-1}$  ( $T > 100\text{ fs}$ ). However, due to laser bandwidth limitation as the spectral regions are not completely probed, the time resolved area normalization analysis (TRANS) couldn't be performed for the clear discrimination of the species in equilibrium. At  $12,400\text{ cm}^{-1}$  excitation frequency, the rate of the decrease in population of species A is faster than the blue edge excitation but the rate of increase in C is almost same. At red edge excitation  $\sim 12,200\text{ cm}^{-1}$ , no population transfer is observed from A to B; whereas the transfer is observed from B to C with less efficiency. The spectral evolution of the time resolved emission spectra (TRES) for different species of IR-140 in ethanol at arbitrary probe delay (T) at different excitation frequencies are shown in [figure S6](#).



## Supplementary Information

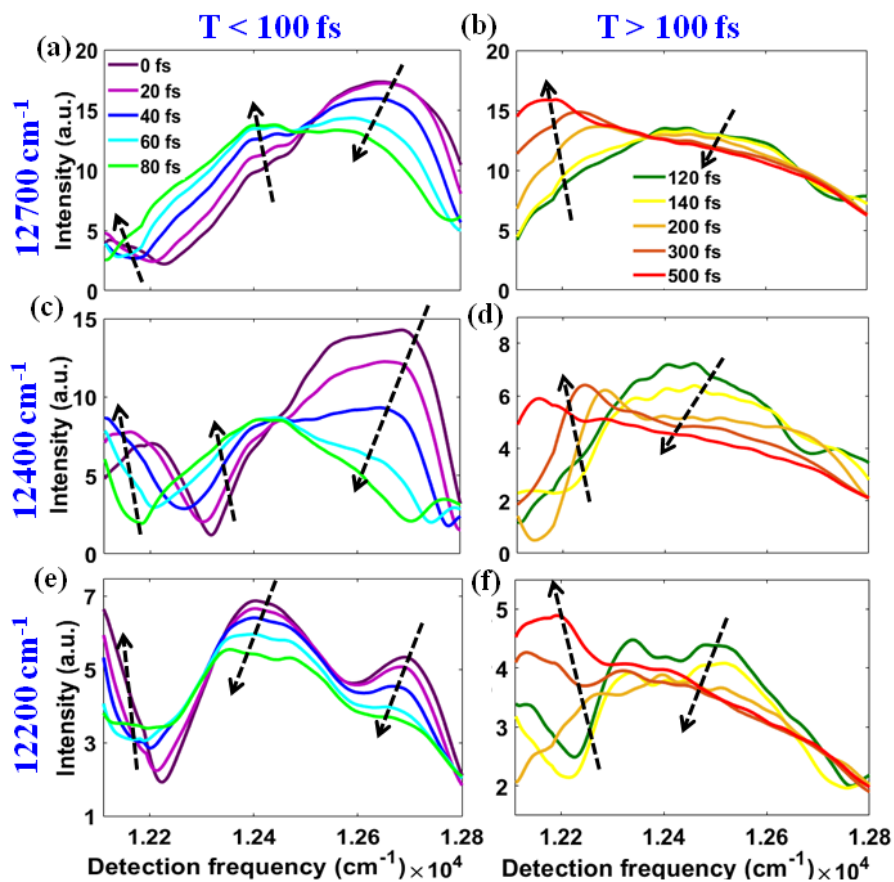


**Figure S6.** Plots of time resolved emission spectra of IR-140 at various probe delays ( $T$ ) in ethanol at excitation frequencies  $\sim 12,700\text{ cm}^{-1}$  (a & b),  $12,400\text{ cm}^{-1}$  (c & d) and  $12,200\text{ cm}^{-1}$  (e & f), respectively. Dotted black arrows show the direction of spectral evolution in different regions.

## Supplementary Information

### [SI-VII]: Spectral evolution of IR-140 at arbitrary probe delays (T):

The spectral evolution for different conformers of IR-140 in ethanol and ethylene glycol at arbitrary probe delay (T) can be seen in [figure S7](#).

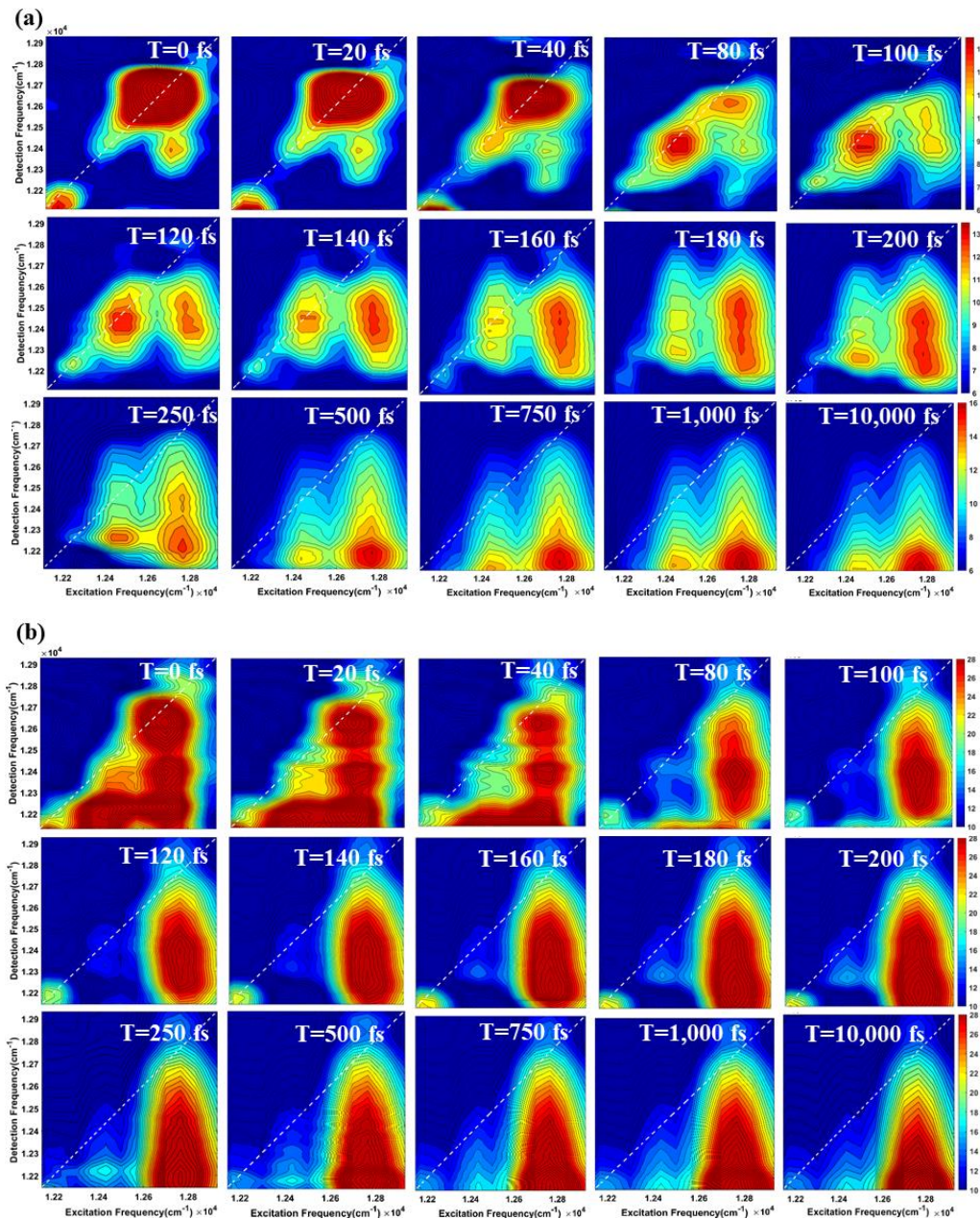


**Figure S7.** Contour plots of 2DES of IR-140 at various probe delays (T) using 2-step phase cycling scheme in ethanol (top panel (a)) and ethylene glycol (bottom panel (b)).



## Supplementary Information

### [SI-VIII]: 2D projection of IR-140 with pump-probe data:

A comparative plot of 2D projection spectra with pump-probe is shown below at 40 fs and 500 fs waiting times.

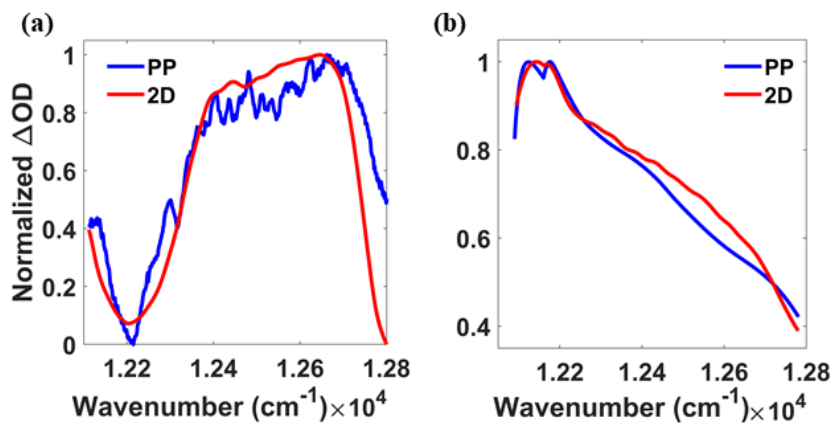


**Figure S8.** Plots of 2D projection along detection axis along with pump-probe spectrum of IR-140 at (a) 40 fs and (b) 500 fs waiting times in ethanol.

## Supplementary Information

### [SI-IX]: Structures of various isomers of IR-140 and DNTTCI:

A series of isomers are observed due to three different single bond rotations in IR 140 and DNTTCI using DFT calculations as shown in [figure S9](#) and [S10](#).

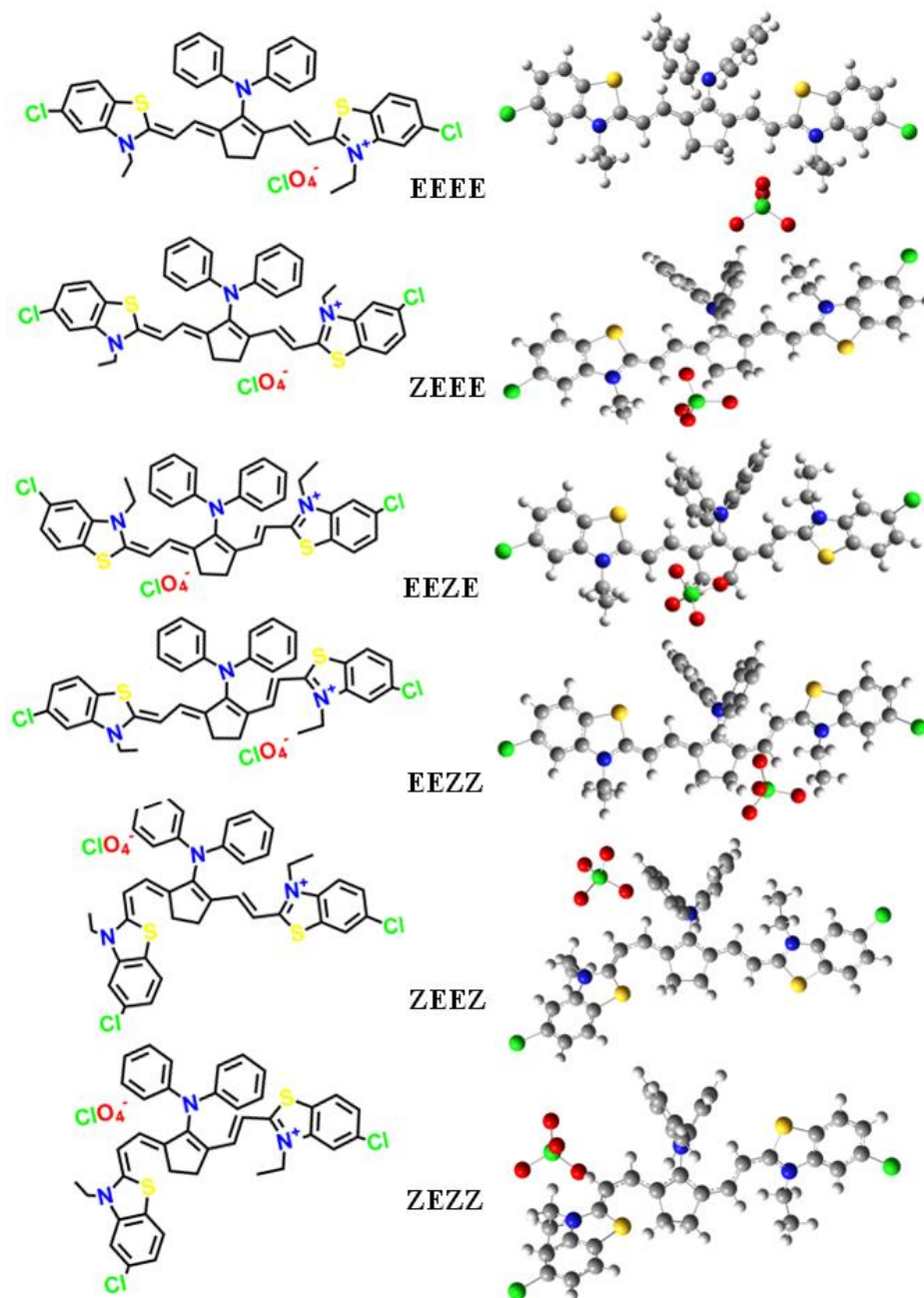


**Figure S9.** DFT-optimized geometries of IR-140 isomers using B3LYP functional and 6-31g basis set. Color: green corresponds to Cl, red to oxygen, yellow to S, blue to N, grey to C and white to H atoms.

## Supplementary Information

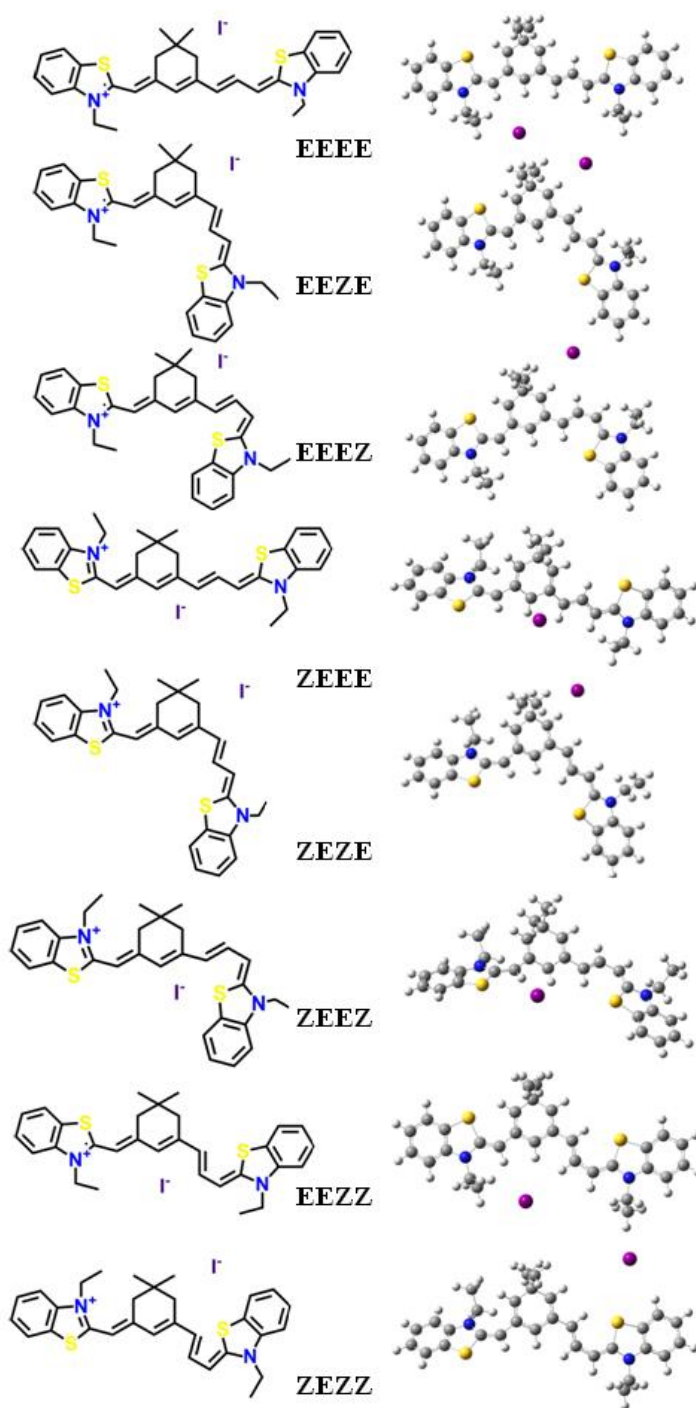


**Figure S10.** DFT-optimized geometries of DNTTCI isomers using B3LYP functional and lanl2dz basis set. Color: violet corresponds to I, yellow to S, blue to N, grey to C and white to H atoms.

## Supplementary Information

### [SI-X]: Data of various parameters for different isomers of IR-140 and DNTTCI:

Species		Electronic (Hartree)	Electronic (Kcal/mol)	Enthalpy (Hartree)	Free energy (Hartree)	Dipole (Debye)	HOMO (Hartree)	LUMO (Hartree)
<b>IR 140</b>	<b>EEEE</b>	-4146.977	- 2612596	-4146.927	-4147.070	24.513	-0.184	-0.127
	<b>EEEZ</b>	-4146.967	- 2612589	-4146.917	-4147.059	21.512	-0.184	-0.126
	<b>EEZE</b>	-4146.966	- 2612589	-4146.917	-4147.055	20.456	-0.184	-0.124
	<b>ZZEE</b>	-4146.961	- 2612585	-4146.911	-4147.053	24.188	-0.183	-0.124
	<b>ZEEZ</b>	-4146.960	- 2612585	-4146.910	-4147.048	28.351	-0.185	-0.127
	<b>ZZEZ</b>	-4146.947	- 2612577	-4146.897	-4147.039	31.377	-0.185	-0.125
<b>DN TT CI</b>	<b>EEEE</b>	-1302.170	- 820367	-1302.134	-1302.245	19.246	-0.187	-0.144
	<b>EEZE</b>	-1302.169	- 820366	-1302.133	-1302.249	27.271	-0.187	-0.145
	<b>EEEZ</b>	-1302.165	- 820364	-1302.129	-1302.239	25.96	-0.190	-0.143
	<b>ZEEE</b>	-1302.158	- 820360	-1302.123	-1302.232	14.883	-0.183	-0.124
	<b>ZEZE</b>	-1302.157	- 820359	-1302.121	-1302.232	21.152	-0.188	-0.146
	<b>ZEEZ</b>	-1302.153	- 820356	-1302.117	-1302.226	9.936	-0.184	-0.115
	<b>EEZZ</b>	-1302.153	- 820356	-1302.117	-1302.226	17.851	-0.189	-0.145
	<b>ZEZZ</b>	-1302.149	- 820354	-1302.114	-1302.224	32.682	-0.191	-0.150

**Table S1.** Zero corrected values of energy, enthalpy, Gibbs free energy and a dipole for DNTTCI and IR-140 isomers calculated by DFT using B3LYP functional, lanl2dz and 6-31 g basis sets, respectively.

## Supplementary Information

### References

- [1] Hunter, J.; White, W. E.; DeLong, K. W.; Trebino, R.; Frequency-resolved optical gating with the use of second-harmonic generation. *J. Opt. Soc. Am. B* **1994**, *11*, 2206-2215.
- [2] Silori, Y.; Seliya, P.; and De, A. K.; Early time solvation dynamics probed by spectrally resolved degenerate pump-probe spectroscopy. *ChemPhysChem* **2019**, *20* (11), 1488-1496.